ISSN 1573-160X, *PHYSICAL OCEANOGRAPHY*, Vol. 31, Iss. 4, pp. 527-538 (2024)
Original Russian Text © V. V. Malinovsky, A. E. Korinenko, 2024,
published in *Morskoy Gidrofizicheskiy Zhurnal*, 2024, Vol. 40, Iss. 4, pp. 576–587

Original article

Investigation of the Wind Wave Breaking Shape Using the Sea Surface Video Records

V. V. Malinovsky ✉, A. E. Korinenko

Marine Hydrophysical Institute of RAS, Sevastopol, Russian Federation
✉ *vladimir.malinovsky@mhi-ras.ru*

Abstract
*Purpose***.** The work is aimed at studying the statistics of width-to-length ratio of a breaking crest for an active phase of wind wave breakings and at assessing the possibility of approximating the geometric shape of a breaking with an ellipse.
Methods and Results. The experimental data including the video records of sea surface and the wind speed measurements were obtained at the stationary oceanographic platform in the Black Sea Hydrophysical Subsatellite Polygon of Marine Hydrophysical Institute (near the village of Katsiveli, the Southern Coast of Crimea) in 2015–2019. Processing the *in situ* data made it possible to form the arrays both of lengths and areas of the breakings and the synchronous measurements of wind speed.
Conclusions. The distributions of random variables proportional to the minor-to-major axes ratios of breakings are obtained. It is shown that these distributions are coincident for the whitecaps of different scales. This fact testifies to the similarity of breaking geometric shapes. The average value of breaking axis ratio obtained from all the data is 0.41. It is concluded that the average geometric shape of the breaking boundaries is satisfactorily described by an ellipse with eccentricity 0.91. The ratio of the speed of a breaking centroid to that of its anterior front is estimated to be 0.9.

Keywords: wind wave breakings, *in situ* studies, distribution of wave breaking lengths, self-similarity of wave breaking geometric form

Acknowledgments: The study was carried out with financial support of the Russian Science Foundation grant No. 24-27-20105, and under the Agreement with the Department of Education and Science of Sevastopol No. 85 dated June 19, 2024.

For citation: Malinovsky, V.V. and Korinenko, A.E., 2024. Investigation of the Wind Wave Breaking Shape Using the Sea Surface Video Records. *Physical Oceanography*, 31(4), pp. 527-538.

Introduction

Many works have been devoted to the results of studies of the statistical characteristics of wind wave breakings. For example, the distributions of the lengths of whitecap ridges obtained as a result of aircraft surveys [1] over the Black Sea were approximated by a gamma distribution. In [2], distributions of whitecap lengths and their speeds were obtained at wind speeds of 5–15 m/s based on the results of four experiments carried out on the FLIP research platform 150 km west of California. Study [3] presents the probability densities of whitecap lengths L, which are well described by the power function $p(L) \sim L^{-2.3}$, and the distribution of the direction of movement of the breakings approximated by the function $A \sim \cos^q$, where q varies from 5 to 4 with an increase in wind speed in the range of 10–16 m/s. The time evolution of the whitecap was studied in [4]. It shows that the wave breaking length and width grow at constant rates proportional to the whitecap speed with coefficients of 0.56 and 0.19, respectively. The relationship between the wave breaking length

and the length of the breaking wave λ is considered in [5], with obtained average ratio $\langle L/\lambda \rangle = 0.1$.

In [1, 6, 7], the sea surface foam area was approximated by ellipses and subsequently the sizes and speeds of whitecap movement were determined. Unfortunately, no justification for such an approximation of wave breaking by an ellipse is given in the abovementioned works. In [8], foam structures were identified using the threshold method. Coordinates of the outer boundary of the selected foam shape were determined to define the breaking area and morphology. Study [8] provides a detailed comparison of the shape method and the ellipse method and shows that both of them give similar results in determining the geometric dimensions and velocities of breakings.

Nevertheless, the question of the type of wave breaking shape approximation remains open to this day. The observed wave breakings during their breaking shape development in the active phase have different shapes – from close to elliptical to "crescent-shaped", when parts of the crest of the breaking wave (mostly short) move at different angles relative to its propagation direction (see Figs. 1 and 2 in [4]). Additional studies of the geometric dimensions of the whitecaps are required to determine the function describing the wave breaking shape.

Note that the width-to-length ratio of the breaking remains insufficiently studied despite the large number of studies on the statistics of the lengths of wing wave breakings and their areas. Such a relationship, if it is constant, will mean that the geometric shape of the whitecap boundaries is self-similar.

Studying the geometric shape of breakings can be important when analyzing data from radar stations installed, for example, on coastal structures or sea vessels. In this case, measurements are carried out at small grazing angles, at which the received signal level is determined by non-Bragg scattering component σ_{nb} formed by breaking wind waves (see [9] and references cited therein). Thus, the study of the whitecap shape and the relationships between their linear sizes will make it possible to develop models of the non-Bragg component of radar scattering.

The work is aimed at studying the width-to-length ratio of a breaking crest for an active phase of wind wave breakings and at assessing the possibility of approximating the geometric shape of a whitecap with an ellipse.

Experimental work area and equipment used

The present study used a database of archival data obtained in the autumn periods of 2015, 2018 and 2019 during full-scale experiments on a stationary oceanographic platform of the Black Sea Hydrophysical Subsatellite Polygon of Marine Hydrophysical Institute (near the village of Katsiveli, Southern Coast of Crimea). The platform is installed approximately 480 m from the shore, the sea depth is ~ 30 m.

Work [5] describes the process of wind wave breaking recording using a video camera. The video camera with a lens providing horizontal viewing angles of 54° and vertical ones of 32° recorded at shooting frequency f_r equal to 25 frames per second, with the 1920 × 1080-pixel resolution. The camera was installed on the platform deck at an altitude of 11.4 m above sea level with a viewing direction of 30–40° to the horizon and 50–60° to the "upwind" direction. The observation geometry ensured no sun glare in the frame.

Wind speed and direction measurements were carried out by the Davis 6152EU complex, which includes a wind speed and direction meter, an air temperature sensor and a water temperature sensor installed at a depth of 3 m. At an altitude of 23 m above sea level, an anemometer was located on the oceanographic platform mast, data from which were recalculated into effective neutrally stratified wind speed *U* at the 10 m height according to method [10].

In situ data were obtained with neutral atmospheric stratification and wind speeds of 5.3–20 m/s.

Data processing method

This work is based on the analysis of a database of archival video sea surface recordings. Pre-processing of *in situ* data was carried out using the algorithm proposed in [11]. The methodology for subsequent calculation of various characteristics of wind wave breaking is described in detail in [3, 5, 12, 13]. Main processing stages required in this work are listed below.

A sign of the whitecap presence in a video frame was a change in the shape of brightness distribution $p(I')$ relative to background distribution $p(I)$ obtained in the absence of foam structures. The surface area where the radiance exceeded a given threshold value was recorded as a breaking. The analysis of time evolution of geometric whitecap foam area characteristics is given in [4, 5, 13], where an algorithm for dividing the breaking process into the active phase and spread foam is considered.

At the final stage of data processing, each pixel of the video frame was tied to coordinates on the horizontal plane taking into account the observation geometry. The intersection point of the optical axis of the lens with the selected plane was taken as the origin of coordinates.

Crest length *L*, occupied area *S*, geometric center coordinates (x_c, y_c) were determined for each whitecap. The temporal evolution of a whitecap moving at a very specific speed is characterized by an increase in *S* and *L*. The maximum values of its area S_m and length L_m are achieved at a time equal to τ, which was considered the breaking lifetime.

Velocity vector components C_c^x and C_c^y were calculated from values $x_c(t), y_c(t)$ for each breaking. The centroid velocity modulus was defined as $C_c = \sqrt{(C_c^x)^2 + \left(C_c^y\right)^2}$. C_c is taken as breaking velocity C_{wb} in this study.

In total, 451,724 breakings were identified when processing video recordings, for each of which the values of S_m, L_m, C_{wb} and τ were recorded in a file.

Estimate of geometric shape of breakings

To consider the breaking shape, we introduce variable η defined as the ratio of minimum axis l_m of the whitecap to length L_m, i.e. $\eta = l_m/L_m$. Axis l_m passes through the breaking centroid perpendicular to L_m. Variable η gives a general idea of the whitecap "elongation". Note that size l_m is only several pixels for small breakings, which will lead to errors in determining l_m. Due to the problems with determining the actual lengths of the minor axis of the whitecap, values l_m were not defined in the present work.

Assume that the breaking area is proportional to the product of its axes: $S_m = \beta L_m l_m$, where β is coefficient depending on the figure approximating the breaking (for example, β = 1 for a rectangle, $\beta = \pi/4$ for an ellipse or circle). Dividing both sides of the indicated expression by L_m^2, we find $S_m/L_m^2 = \beta\eta$. Variables S_m and L_m are random values obtained as a result of *in situ* measurements for each breaking. Consequently, it is not difficult to calculate the statistical characteristics of random variable S_m/L_m^2 coinciding with βη. Note that random variable here is η, while coefficient β is some constant, which can take different values for different breakings in the general case. At the same time, both β and η are considered at this stage as unknown variables.

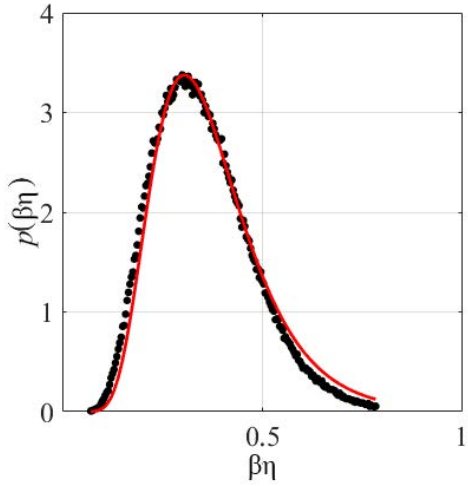

F i g. 1. Probability density of all the measured values of βη. Solid red line is calculated by function (1)

Consider probability density $p(\beta\eta)$. Figure 1 shows its distribution obtained for all measured values S_m/L_m^2 by black dots. The probability density is satisfactorily described by the function shown in Fig. 1 by red line:

$$p(\beta\eta) = b\exp\left[-a\ln^2\left(d\frac{\beta\eta}{\eta_0}\right)\right], \quad (1)$$

where a = 0.69, b = 3.39, d = 0.87. These coefficients were obtained using the least squares method. Coefficient $\eta_0 = 0.35$ was defined as the average of all found values S_m/L_m^2. Note that the deviation of the average value $\langle\beta\eta\rangle = \int_0^m (\beta\eta)p(\beta\eta)d(\beta\eta)$ equal to 0.365, does not exceed 4% from η_0 (m is the maximum value of βη).

Note that type of distribution (1) was not chosen randomly, but due to the fact that the probability density is close to a parabola on a double logarithmic scale

$$\ln[p(\beta\eta)] = B - a[\ln(\beta\eta) - \ln(\eta_0/d)]^2.$$

Since coefficient β, as mentioned above, can take different values for different scales of breaking, behavior of $p(\beta\eta)$ for different C_{wb} and τ is to be estimated.

Really, as shown in [5], the distribution of ratio L_m to breaking wave length λ is quite "narrow" and $\langle L_m \rangle = 0.1\lambda$. Assuming that whitecap speed is equal to breaking wave speed, we obtain $\langle L_m \rangle \sim C_{wb}^2$. Thus, the maximum breaking length depends on C_{wb}. However, the relationship between S_m / L_m^2 and C_{wb} is not obvious.

Let us determine the distributions of $p(\beta\eta)$ at various observed whitecap speeds. The range of all measured C_{wb} (1–8 m/s) is divided into three intervals with a step $\Delta C_{wb} = 2.5$ m/s. In Fig. 2, *a*, symbols show the distributions of $p(\beta\eta)$ in selected intervals of breaking rates (numbers in the legend). All probability densities $p(\beta\eta)$ coincide practically and the entire set of points is satisfactorily described by function (1) shown by the red line.

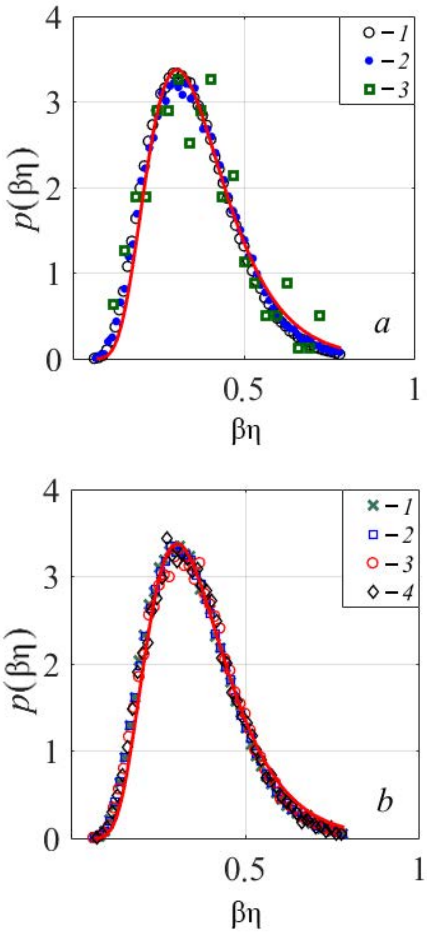

F i g. 2. Probability densities of the measured variables of βη: *a* – in the intervals of wave breaking velocities, m/s (*1* – $1 \le C_{wb} \le 3.5$; *2* – $3.5 \le C_{wb} \le 6$; *3* – $6 \le C_{wb} \le 8$); *b* – in the intervals of whitecaps lifetime, s (*1* – $0.16 \le \tau \le 0.56$; *2* – $0.56 \le \tau \le 0.96$; *3* – $0.96 \le \tau \le 1.36$; *4* – $1,36 \le \tau \le 1.76$)

Of interest are distributions p(βη) calculated for different breaking lifetime. As shown in [4], the values of the maximum whitecap lengths grow linearly in time at a rate of $C_L = 0.56C_{wb}$ and reach their maximum at $t = \tau$. Thus, the breaking lifetime determines value L_m. Let us divide the range of all measured τ (0.16–1.8 s) into four intervals with a step of $\Delta\tau$ = 0.4 s. In Fig. 2, *b*, symbols show the distributions of $p(\beta\eta)$ in selected intervals τ (numbers in the legend). Here, as in Fig. 2, *a*, all probability densities $p(\beta\eta)$ coincide and are well described by function (1) shown by the red line.

Average characteristics of distribution $p(\beta\eta)$ are considered below. In Fig. 3, *a*, squares show the values of $\langle\beta\eta\rangle$ in the studied intervals, the solid line corresponds to the average value of η_0 equal to 0.35.

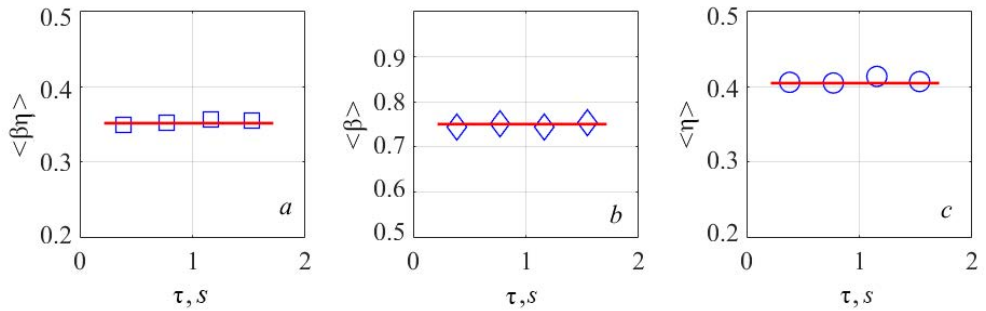

F i g. 3. Dependencies of mean characteristics of probability distribution $p(\beta\eta)$ on wave breaking lifetime: first moment (*a*); coefficient β (*b*); wave breaking axis ratio (*c*)

Standard deviation of population $\langle\beta\eta\rangle$ from η_0 is 0.003, which confirms the coincidence of distributions $p(\beta\eta)$ for different scales of breakings.

To estimate coefficient β, distribution normalization condition (1) is used:

$$\int_0^m p(\beta\eta)d(\beta\eta) = 1. \quad (2)$$

It will be assumed that η theoretically varies within $0 \le \eta \le 1$ and takes a value equal to zero when only the leading front breaks without foam generation behind it, and equal to one in the case when the major and minor whitecap axes coincide (for example, for a circle). Since in our assumption coefficient β is constant and can take different values for different scales of breakings, expression (2) is written in the following form:

$$\beta\int_0^1 p(\beta\eta)d\eta = 1.$$

Then, integrating over η, we obtain

$$\frac{1}{2}\sqrt{\frac{\pi}{a}}\frac{b\eta_0}{d}\exp\left(\frac{1}{4a}\right)\left[1+\operatorname{erf}\left(\frac{2a\ln\left(d\frac{\beta}{\eta_0}\right)-1}{2\sqrt{a}}\right)\right] = 1. \quad (3)$$

Coefficient β can be estimated using the obtained formula. Setting its initial value equal to β_0, we calculate the difference modulus between the left side, which we denote as *f*, and the right side in the specified formula. Next, using the iteration

method, taking into account the sign of difference $f-1$, increment $\Delta\beta_j$ and $\beta_{j+1}=\beta_j+\Delta\beta_j$ is determined until value $f-1$ will be established up to given $|f-1|\le\epsilon$. In the present calculations, $\epsilon=10^{-5}$ was specified.

In Fig. 3, *b*, diamonds show estimates of β calculated using formula (3) for distributions in considered intervals τ. Values β have a small spread and cluster around a mean ⟨β⟩ of 0.75 (solid line). The behavior of ⟨η⟩ in different βη intervals requires separate consideration.

Taking into account that $\beta\approx\text{const}$ and using found value β⟨η⟩ presented in Fig. 3, *a*, it is not difficult to determine the average value of the ratio of the breaking axes. In Fig. 3, *c*, ⟨η⟩ in the above τ intervals is shown by circles, the solid line corresponds to expression $\langle\eta\rangle=0.41$; values ⟨η⟩ are grouped around straight line ⟨η⟩ with a standard deviation of 0.006.

The above results show that the average ratio of the breaking axes is the same regardless of its scale when analyzing the entire data set obtained. In this case, we can talk about the self-similarity of the breaking geometric shape.

Until now, the analysis was based on the array of measured random values S_m and L_m and their ratios $S_m/L_m^2=\beta\eta$. If we use the values of the semi-axes instead of L_m and l_m, the expression for the breaking area will be written as follows

$$S_m=4\beta(L_m/2)^2\eta. \tag{4}$$

Taking into account the results obtained above, 4β is equal to 3, which is only 4.7% less than value π. Thus, formula (4) describes the ellipse area quite satisfactorily.

Discussion of results

Aforementioned probability densities *p*(βη) shown in Figs. 1 and 2 and values η_0 should be considered as average dependencies obtained for the characteristics of all breakings during their lifetime.

In the present work, a specific geometric shape of a whitecap was not initially determined when studying the statistical characteristics of breakings. The only assumption was that the breaking area was proportional to the product of its major and minor axes. This proportionality coefficient value makes it possible to evaluate the possibility of whitecap approximating with a specific geometric figure.

In our opinion, the value of proportionality coefficient $\beta\approx\pi/4$ obtained in this work in formula (4) is significant. It can be said then that the breaking boundaries are described by an ellipse.

It is of interest to compare the results obtained in this work and earlier. In [4], the growth rates of breaking axes during their lifetime are considered, and these rates are almost constant: $C_l=0.19C_{wb}$ for the minor axis of a whitecap, $C_L=0.56C_{wb}$ for the major axis. In this work, the maximum values of breaking axes are defined as $l_m=C_l\tau$ and $L_m=C_L\tau$, then ratio l_m/L_m is 0.34, which is 20% different from ⟨η⟩ obtained in this work equal to 0.41. It should be noted here that ratio ⟨η⟩ does not depend on the scale of whitecaps according to the results of this work and work [4].

As shown above, since the boundaries of breakings are satisfactorily described by an ellipse, η can be determined by formula $\eta=\sqrt{1-\varepsilon^2}$, where ε is average

eccentricity of breakings. Few works present dependence ⟨ε⟩ on wind speed. To compare our data with the results of other authors, the range of wind speeds is divided into 6 intervals with a step $\Delta U = 2.5$ m/s and average wind speed values $\langle U \rangle$ in them.

In Fig. 4, squares show the wind dependence of our calculated ε, the solid line shows the average value ⟨ε⟩ equal to 0.91; light circles correspond to the data of [1], dark circles – to the data of [14].

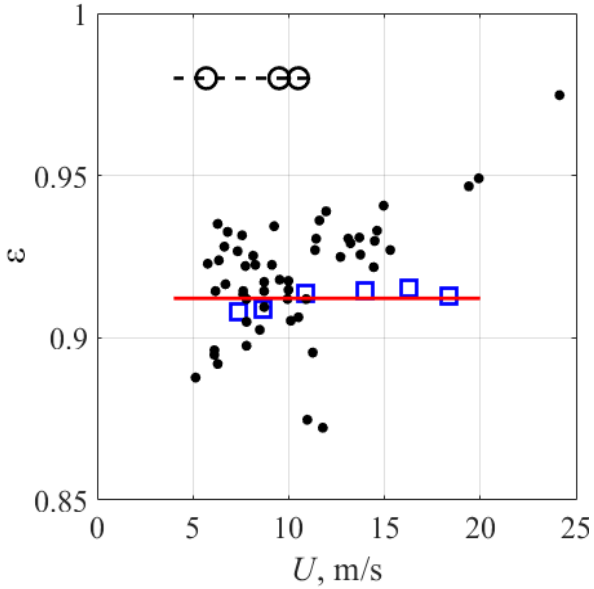

F i g. 4. Dependence of eccentricity on wind speed when approximating the wave breaking with an ellipse

The obtained eccentricity estimate is consistent with average value ⟨ε⟩ equal to 0.9 and calculated for an array of whitecaps generated by winds with a speed of 5–24 m/s [14]. According to the results of aircraft measurements of breakings [1], $\langle \varepsilon \rangle = 0.98 \pm 0.007$ at U = 5.7–10.5 m/s, which is significantly greater than results obtained in this research. A possible reason for the increased eccentricity value in [1] can be inaccuracy in determining the minor breaking axis, which varies in the range of 0.39–0.56 m (see Table 1 and Fig. 3, a in [1]) with spatial resolution of measurements 0.2 m.

In [1, 14], the eccentricity value was determined by approximating the breaking by an ellipse, whereas in the present case, estimate ⟨ε⟩ was obtained without initially determining the whitecap shape. Note that, as in the aforementioned works, value ⟨ε⟩ does not change under different observation conditions.

The results obtained in this work indicate that the breakings geometric shape is self-similar. This conclusion can be useful for the development of models describing the non-Bragg radar signal component. Indeed, σ_{nb} is determined by sea surface fraction Q covered by breakings in [15]. If $L = \int \Lambda(\mathbf{k}) d\mathbf{k}$ is total length of breaking crests on a sea surface unit, then Q will be proportional to $k^{-1}\Lambda(\mathbf{k})d\mathbf{k}$ under

the condition of a self-similar form of breakings. The proportionality coefficient was determined by comparing model σ_{nb} with radar measurement data in [15]. The results of this work will further make it possible to estimate the proportionality coefficient relating σ_{nb} to the wind wave breaking size.

When determining the velocities of different whitecap sections, the above values η and the elliptical shape of the breakings are important. Of interest is the ratio of C_{wb} to phase velocity of the breaking wave.

In [5, 12], it is assumed that the centroid speed is equal to phase velocity of the breaking wave, $C_c = c$, while in [2] $C_c = 0.9c$. During laboratory studies, the whitecap crest speed was measured and it was found that C_c = (0.8–0.9) *c* [16].

At the same time, the author understood the breaking movement speed as the movement speed of its front C_f in [17]. If the front is understood as the breaking boundary leading in the direction of movement, then its speed and the speed of the centroid will differ, since coordinates (x_c, y_c) are determined in the entire foam structure area.

As the whitecap area increases, the length of its minor axis in the direction of movement also increases and, therefore, leading front speed C_f must exceed C_c.

Let us estimate breaking ratio C_c to its front speed C_f. Here, C_f is understood as the movement speed of the intersection point of the minor axis of the ellipse with the breaking leading front. Let us choose a coordinate system in which axis *x* coincides with the breaking movement direction. At time *t*, coordinate x_f is defined as $x_f(t) = x_c(t) + l(t)/2$, and the distance covered by the whitecap front during time Δ*t* will be as follows

$$x_f(t + \Delta t) - x_f(t) = x_c(t + \Delta t) - x_c(t) + [l(t + \Delta t) - l(t)]/2. \quad (5)$$

Dividing the left and right sides of this equation by Δ*t*, the following expression including C_c and C_f is obtained:

$$C_f = C_c + 0.5C_l, \quad (6)$$

where C_l is increase rate *l* in the interval $(t, t + \Delta t)$. Given the definition of η, it can be written that $C_l = \eta C_L$. Then, using expression $C_L = 0.56C_c$ from [4] and dividing the left and right sides of equation (6) by C_c, we obtain

$$C_c = C_f/[1 + 0.28\eta]. \quad (7)$$

Thus, if it is assumed that the phase velocity of the breaking wave coincides with C_f [17], then, as follows from formula (7), the whitecap centroid velocity is less than the leading front velocity. When using value $\langle\eta\rangle = 0.41$ obtained above, the speed ratio is $C_c/C_f \cong 0.9$. This can be significant, for example, when calculating dissipation of wave energy $E_D \sim \int_0^\infty c^5\, \Lambda dc$ Λdc associated with breakings. If the dissipation energy is written as $E_D^f \sim \int_0^\infty C_f^5\ \Lambda dC_f$ for the speed of the breaking leading front and as $E_D^c \sim \int_0^\infty C_c^5\ \Lambda dC_c$ for the centroid speed, then $E_D^f = 1.88E_D^c$.

Conclusion

This work examines the statistical characteristics of the ratio of the minor-to-major axes of wind wave breaking. The analysis was carried out using an experimental data set including 451,724 identified breakings, which were obtained by processing video recordings of the sea surface. The studies were carried out at wind speeds of 5.3–20 m/s. Its lifetime, the speed of centroid movement, as well as the maximum area and maximum length along the breaking wave crest were determined for each individual whitecap.

In general, breakings have a complex geometric shape. Initially, we did not make any assumptions about the geometric shape of its boundaries, for example, in the form of an ellipse. The only hypothesis was that the whitecap area was proportional to product $\beta\eta$, where β is certain coefficient, η is random variable representing the ratio of the breaking axes (minimum to maximum).

It is shown that the probability densities of random variable $\beta\eta$ coincide practically in all observed intervals of τ and breaking rates. Thus, distribution $\beta\eta$ is universal for breakings of various scales and $\langle\beta\eta\rangle$ is equal to 0.35, where β and η are unknown variables.

Using distribution normalization condition $p(\beta\eta)$, required parameters β and $\langle\eta\rangle$, equal to 0.75 and 0.41, respectively, were determined using the iterative method. Almost constant value $\langle\eta\rangle$ obtained for different sizes of whitecaps gives grounds to speak about the self-similarity of the breaking geometric shape.

The results obtained show that value 4β coincides with π with an accuracy of $\sim 4\%$ and, therefore, the breaking geometric shape is quite satisfactorily described by an ellipse. It was found that the average eccentricity value is 0.91 and does not change under different observation conditions.

The work provides an estimate of the whitecap leading front speed. It is shown that it is 10% higher than the speed of the breaking centroid.

REFERENCES

1. Bondur, V.G. and Sharkov, E.A., 1986. Statistical Characteristics of Linear Elements of Foam Formations on the Sea Surface as Derived from Optical Sounding Data. *Issledovanie Zemli iz Kosmosa*, (4), pp. 21-31 (in Russian).

2. Gemmrich, J.R., Banner, M.L. and Garrett, C., 2008. Spectrally Resolved Energy Dissipation Rate and Momentum Flux of Breaking Waves. *Journal of Physical Oceanography*, 38(6), pp. 1296-1312. https://doi.org/10.1175/2007JPO3762.1

3. Korinenko, A.E., Malinovsky, V.V. and Kudryavtsev, V.N., 2018. Experimental Research of Statistical Characteristics of Wind Wave Breaking. *Physical Oceanography*, 25(6), pp. 489-500. https://doi.org/10.22449/1573-160X-2018-6-489-500

4. Korinenko, A.E. and Malinovsky, V.V., 2023. Field Investigations of the Geometric Features of Wind Wave Breaking. *Physical Oceanography*, 30(6), pp. 776-791.

5. Korinenko, A.E., Malinovsky, V.V., Kudryavtsev, V.N. and Dulov, V.A., 2020. Statistical Characteristics of Wave Breakings and Their Relation with the Wind Waves' Energy Dissipation Based on the Field Measurements. *Physical Oceanography*, 27(5), pp. 472-488. https://doi.org/10.22449/1573-160X-2020-5-472-488

6. Sharkov, E.A., 2007. *Breaking Ocean Waves: Geometry, Structure, and Remote Sensing*. Berlin, Heidelberg: Springer, 278 p. https://doi.org/10.1007/978-3-540-29828-1

7. Schwendeman, M.S. and Thomson, J., 2017. Sharp-Crested Breaking Surface Waves Observed from a Ship-Based Stereo Video System. *Journal of Physical Oceanography*, 47(4), pp. 775-792. https://doi.org/10.1175/JPO-D-16-0187.1

8. Kleiss, J.M. and Melville, W.K., 2011. The Analysis of Sea Surface Imagery for Whitecap Kinematics. *Journal of Atmospheric and Oceanic Technology*, 28(2), pp. 219-243. https://doi.org/10.1175/2010JTECHO744.1

9. Malinovsky, V.V., Korinenko, A.E. and Kudryvtsev V.N., 2018. Empirical Model of Radar Scattering in the 3-cm Wavelength Range on the Sea at Wide Incidence Angles. *Radiophysics and Quantum Electronics*, 61(2), pp.98-108. https://doi.org/10.1007/s11141-018-9874-7

10. Fairall, C.W., Bradley, E.F., Hare, J.E., Grachev, A.A. and Edson, J.B., 2003. Bulk Parameterization of Air-Sea Fluxes: Updates and Verification for the COARE Algorithm. *Journal of Climate*, 16, pp. 571-591. https://doi.org/10.1175/1520-0442(2003)016<0571:BPOASF>2.0.CO;2

11. Mironov, A.S. and Dulov, V.A., 2008. Detection of Wave Breaking Using Sea Surface Video Records. *Measurement Science and Technology*, 19(1), 015405. https://doi.org/10.1088/0957-0233/19/1/015405

12. Dulov, V.A., Korinenko, A.E., Kudryavtsev, V.N. and Malinovsky, V.V., 2021. Modulation of Wind-Wave Breaking by Long Surface Waves. *Remote Sensing*, 13(14), 2825. https://doi.org/10.3390/rs13142825

13. Pivaev, P.D., Kudryavtsev, V.N., Korinenko, A.E. and Malinovsky, V.V., 2021. Field Observations of Breaking of Dominant Surface Waves. *Remote Sensing*, 13(16), 3321. https://doi.org/10.3390/rs13163321

14. Mironov, A.S. and Dulov, V.A., 2008 Statistical Properties of Individual Events and Energy Dissipation of Breaking Waves. *Ecological Safety of Coastal and Shelf Zones and Comprehensive Use of Shelf Resources*, (16), pp. 97-115 (in Russian).

15. Kudryavtsev, V.N., Hauser, D., Caudal, G. and Chapron, B., 2003. A Semiempirical Model of the Normalized Radar Cross-Section of the Sea Surface 1. Background Model. *Journal of Geophysical Research: Oceans*, 108(C3), 8054. https://doi.org/10.1029/2001JC001003

16. Banner, M.L. and Peirson, W.L., 2007. Wave Breaking Onset and Strength for Two-Dimensional Deep-Water Wave Groups. *Journal of Fluid Mechanics*, 585, pp. 93-115. https://doi.org/10.1017/S0022112007006568

17. Phillips, O.M., 1985. Spectral and Statistical Properties of the Equilibrium Range in Wind-Generated Gravity Waves. *Journal of Fluid Mechanics*, 156, pp. 505-531. https://doi.org/10.1017/S0022112085002221

Submitted 22.04.2024; approved after review 02.05.2024;
accepted for publication 16.05.2024

About the authors:

Vladimir V. Malinovsky, Senior Researcher, Marine Hydrophysical Institute of RAS (2 Kapitanskaya Str., Sevastopol, 299011, Russian Federation), CSc. (Phys.-Math.), **ORCID ID: 0000-0002-5799-454X**, **ResearcherID: F-8709-2014**, **Scopus Author ID: 23012976200**, vladimir.malinovsky@mhi-ras.ru

Aleksandr E. Korinenko, Senior Researcher, Marine Hydrophysical Institute of RAS (2 Kapitanskaya Str., Sevastopol, 299011, Russian Federation), CSc. (Phys.-Math.), **Scopus Author ID: 23492523000, ORCID ID: 0000-0001-7452-8703**, korinenko.alex@mhi-ras.ru

Contribution of the co-authors:

Vladimir V. Malinovsky – development of experimental research method, analysis and synthesis of research results, preparation of the paper text

Aleksandr E. Korinenko – development of techniques and carrying out the experimental studies, participation in the discussion of the article materials, analysis and synthesis of the research results

The authors have read and approved the final manuscript.
The authors declare that they have no conflict of interest.